APPLICATION NOTE

CELLINK
A BICO COMPANY

A 3D Bioprinted Model of Multicellular Lung Cancer Assembloids

Shubhankar Nath, PhD, Himjyot Jaiswal, PhD, Itedale Namro Redwan, PhD

CELLINK LLC, Boston, US

Abstract

Three-dimensional cancer models such as spheroids, tumoroids and organoids have become common tools for preclinical drug development. However, a major limitation of these models is the lack of a native microenvironment where cell-cell communications and cellular migrations take place within an extracellular matrix (ECM)-based stroma. Establishing this native tumor microenvironment is critical for better understanding disease progression and developing robust drug discovery studies. In the present study, a multicellular 3D bioprinted lung cancer assembloid model was developed by incorporating human lung cancer cells (A549), lung adenocarcinoma-associated fibroblasts and human umbilical vein endothelial cells (HUVECs) in a laminin-collagen-rich stromal environment. Using genetically encoded fluorescent cancer cells, the migration of cancer cells and merging of cancer spheroids within the matrix were visualized and further confirmed by histological analysis of fixed assembloids within the bioprinted constructs. Immunofluorescent staining was conducted to verify the expression of cell-surface and intracellular markers of 3D lung cancer tissue. Furthermore, this study demonstrates that the embedded cancer cells expressed PD-L1, implying the suitability of such assembloid models for *in vitro* immunotherapy studies. The model and analysis protocols described here could be easily adapted for other cancer and healthy tissue models, in applications such as developmental biology, regenerative medicine and toxicology.

Introduction

In vitro 3D tissue or tumor models refer to the spheroids and organoids that healthy or cancerous cells rearrange themselves into to form 3D structures that partly mimic *in vivo* tissue morphology. These 3D models have extensively been used for drug screening and regenerative medicine studies because of their simplicity and ease of use. However, a major limitation of these models is their lack of a native microenvironment where various cell-cell communications and cellular migrations occur within an ECM-embedded stroma. For example, spheroid models used for drug testing are often developed with a single cancer cell line and do not reflect the effect of other cell populations, such as cancer-associated fibroblasts (CAFs), immune cells and endothelial cells, all of which generally exist in a native tumor microenvironment. The behavior of cancer cells is altered due to their interaction with the adjacent matrix (Bissell, 2001), cells and biological factors (molecules, cytokines, hormones, etc.). Studies have also shown that cancer cells respond to drugs differently in the presence of CAFs (Sahai, 2020). Thus, it is important to consider the contribution of other stromal components when fabricating 3D tumor or tissue models.

Assembloids are next-generation 3D tissue models that overcome these limitations. The term assembloid refers to a 3D reconstruction of matrix-embedded, multicellular, multiregional tissue architecture that structurally and functionally mimics certain aspects of the native *in vivo* tissue or organ. Assembloids are useful tools to examine cellular migration and connections that are often

necessary for developing tissue and organs, such as the brain. Several recent studies on brain assembloids have shown previously inaccessible facets of neurobiology and how neurons interact in healthy and diseased cerebral tissue (Andersen, 2020; Marton, 2020; Miura, 2020).

Although research with tumor assembloids is still in its infancy, a recent report described the development of bladder cancer assembloids using patient-derived tumor cells with matching stromal cells, such as endothelial cells, CAFs, immune and muscle cells (Kim, 2020). Kim's finding, that the tumor plasticity is governed epigenetically through the interactions with the associated stroma, could not have been identified using any other 3D model.

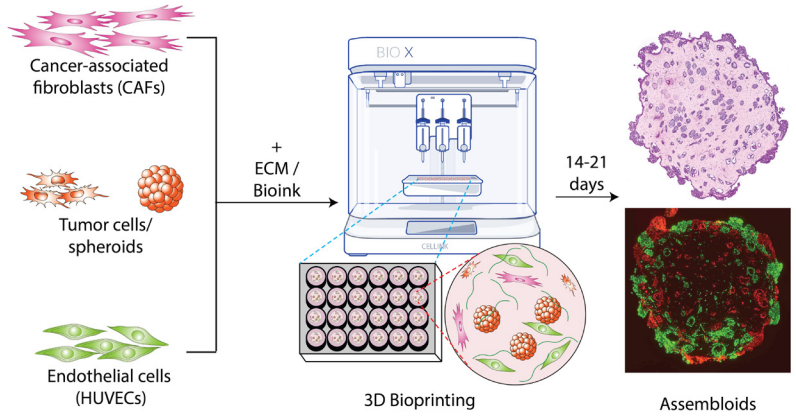

Figure 1. Overview of lung cancer assembloid development. *Cancer cell-derived spheroids are mixed with matched cancer-associated fibroblast and endothelial cells, and bioprinted in the presence of an ECM-based bioink. The bioprinted 3D constructs are maintained under appropriate growth conditions for 14 to 21 days to develop assembloids.*

In the present study, 3D bioprinted lung cancer assembloids were developed by incorporating A549 cells, primary CAFs from lung adenocarcinoma patient, and HUVECs in a laminin-collagen-rich stromal environment (**Figure 1**). Genetically encoded fluorescent cancer cells were used to mimic a multiregional lung tumor and to visualize the migration of cancer cells and the merging of cancer spheroids within the matrix. This visualization was then confirmed by histological analysis of fixed assembloids within the bioprinted constructs. Immunofluorescent staining was conducted to verify the expression of cell-surface and intracellular markers of 3D lung cancer tissue. Furthermore, the study demonstrated that the embedded cancer cells expressed PD-L1, suggesting the suitability of such assembloid models for *in vitro* immunotherapy studies. The model and analysis protocols described here could easily be adapted for other cancer or healthy tissue models in applications such as developmental biology, regenerative medicine and toxicology.

Materials and methods

Cell preparation

Human lung cancer A549 cell line (ATCC, CCL-185) was cultured in 2D T75 flasks with RPMI 1640 medium (Gibco, 22400-089) supplemented with 10% fetal bovine serum (Gibco, 10270-106), 100 U/mL penicillin and 100 µg/mL streptomycin (Thermo Fisher, 15140122). The cells were subcultured every 3 to 4 days. For live cell imaging, GFP and mCherry expressing stable A549 cell lines were created by transducing lentiviruses encoding a GFP or mCherry gene as previously described (Kercher, 2020). The cells with similar fluorescent properties were isolated using a FACSAria (BD Biosciences) cell sorter and expanded before cryopreservation or directly used in the following cell studies.

HUVECs (Lonza, C2519AS) were maintained in EBM-2 basal medium (Lonza, CC-3156) supplemented with EGM-2 SingleQuots Kit (Lonza, CC-4176). Primary CAFs (Neuromics, CAF07-AD) were cultured in FGM-2 fibroblast growth media (Lonza, CC-3132). All cells were grown at 37°C in 75 cm² tissue culture flasks in a humidified incubator with 5% CO_2. The cells were harvested using Accutase and washed once in DPBS before being used in the biofabrication process.

Spheroid formation with Sphericalplate 5D

Kugelmeiers Sphericalplate 5D plates were used to create A549 spheroids of consistent size. The plate contains 750 microwells per well, which yields a total of 9,000 spheroids per plate. First, the Sphericalplate 5D was prepared by incubating the plate at 37°C for 15 minutes with 1 mL of RPMI growth media in each well. The plate was then centrifuged at 200*g* for 4 minutes to remove any

trapped air bubbles, and visual confirmation was obtained under an inverted light microscope. The plate and existing growth media were returned to the incubator while the cells were being prepared. The A549 single-cell suspension was prepared with a cell density of 750,000 cells/mL of medium. One milliliter of cell suspension was added to each spheroid well. The plate was then incubated for 2 days without disruption, allowing spheroids to form. The media was not changed during this process. After 2 days, spheroids were collected by gently swirling the plate and pipetting the spheroid suspension using a large orifice 1 mL pipette tip. The spheroid suspension was collected in a 15 mL conical tube to allow the spheroids to sediment by gravity for 15 minutes. The supernatant was carefully removed, and the spheroids were collected for bioprinting as described in the next section. A similar process was followed for both wild type (non-fluorescent) and fluorescent (GFP or mCherry expressing) A549 cells/spheroids.

Bioink preparation and bioprinting

A custom bioink was prepared by mixing neutralized Coll 1 (CELLINK, IKD119261001, 10 mg/mL) and Growth Factor Reduced Matrigel (Corning, 354234, 10 mg/mL) at a ratio of 1:1 (v/v) to reach the desired collagen and laminin concentration needed to develop this lung tumor model. In parallel, 3 x 10^6 of CAFs and 3 x 10^6 of HUVECs were also harvested and co-pelleted in a 15 mL Falcon tube.

The cell pellet was resuspended in 1 mL of the custom bioink to achieve a homogeneous distribution of the cells before the bioink-cell suspension was mixed with 9,000 spheroids/mL of bioink. Large orifice pipette tips were used for cell-bioink mixing to reduce shear stress and keep the spheroids intact. The bioink suspension was then carefully loaded into a 3 mL cartridge and bioprinted as droplets in an ultra-low attachment 24-well plate (Corning, 3473) following the standard Coll 1 Bioprinting Protocol. Each droplet volume was about 40 µL. The droplets were cured by incubating at 37°C for 30 minutes. Then, 2 mL of a custom growth media (RPMI: EGM: FGM-2; 1 :2 :2; v/v) was added to each well. All cultures were maintained at 37°C and 5% CO_2 for 21 days with media refreshment every 2 to 3 days.

Histology and immunostaining

The 3D constructs were fixed with a final concentration of 4% paraformaldehyde (Electron Microscopy, 15710) overnight in the presence of 30% sucrose in an aqueous solution. The constructs were dehydrated, embedded in paraffin, cut into 7 µm thick sections and stained for H&E, according to standard histological protocols. For immunostaining, the sections were first deparaffinized by heating at 60°C for 1 hour, followed by two incubations of 10 minutes each in pure xylene at room temperature. The tissue samples were then rehydrated by incubating in gradient ethanol solutions (100%, 95%, 70%, respectively). The antigens were retrieved by incubating the slides in a citrate buffer (Sigma, C999, 1X) at pH 6.5 and a temperature of 98°C. The samples were then permeabilized using 0.1% TBS-Triton X-100 for 15 minutes followed by washing in distilled water. They were then blocked with 5% goat serum and 0.5% Tween-20 in PBS at room temperature for 30 minutes. Primary and secondary antibodies were diluted in blocking solution to achieve the recommended antibody concentration. The primary and secondary antibodies were incubated overnight at 4°C and for 1 hour at room temperature, respectively. The following antibodies were used for immunofluorescent staining: E-cadherin, α-smooth muscle actin (α-SMA), CD93, PD-L1 and Ki-67. Coverslips were mounted with ProLong Diamond antifade mountant with DAPI (Thermo Fisher, P36962) and cured overnight before the slides were sealed with transparent nail polish for long-term preservation.

Image acquisition and processing

H&E images were taken using the NanoZoomer S360 (Hamamatsu, C13220-01) with 4X, 20X and 40X objective lens and edited using NDP.view2 software. Fluorescent images were captured using either a Nikon epifluorescence microscope or an Olympus FV1000 MPE multiphoton confocal microscope. Images were edited with Fiji software and assembled with Adobe Illustrator.

Results and discussion

Development of assembloids and viability studies

First, wild type and fluorescent (GFP- and mCherry-expressing) A549 cells were cultured in spherical plates to create hundreds of uniform cancer spheroids (**Figure 2A-C**). The spheroids reached about 200 µm in diameter after 48 hours. Cancer spheroids were harvested and mixed with HUVECs and CAFs in the presence of a custom bioink. The cell mix was then bioprinted onto a 24-well plate using the BIO X. Bright-field microscopy confirmed the structural integrity of the spheroids immediately after the bioprinting process (**Figure 2D**). Cellular viability was determined on days 1, 7, 14 and 21 by staining with calcein and propidium iodide. The overall viability of the cells in an assembloid was always more than 86% compared to the day 1 baseline (data not shown). Starting on day 7, fusion and connection between embedded spheroids were observed (**Figure 2E**, inset, pink arrowhead). To further characterize the proliferative state of the assembloids, a few samples were fixed on day 21 and embedded in paraffin. Immunostaining for Ki-67 indicated that the cells and spheroids embedded within the assembloid structure were in an active proliferative state as shown in **Figure 2F**. Cells located at the periphery of the assembloids expressed more Ki-67 compared to the ones in the inner core, probably due to increased accessibility to gas and nutrients.

Migration of cells and fusion of spheroids

Assembloids are often characterized by visualizing the cell migration patterns and intercellular connections with other cells within the structure. To study whether this also happens in this lung cancer assembloid model, GFP- and mCherry-expressing A549 spheroids were used to create the assembloid structures along with other non-fluorescent cells (CAFs and HUVECs). For better visualization of the spatially distributed spheroids in a large assembloid structure (>3 mm diameter), a few fluorescent A549 cell-containing assembloids were fixed and embedded in paraffin on day 21. Following deparaffinization, slices were imaged using a fluorescent microscope with or without DAPI counterstaining. **Figure 3A-B** shows multiple instances of spheroid fusion and migration of GFP or mCherry-expressing A549 cells toward each other (yellow arrows).

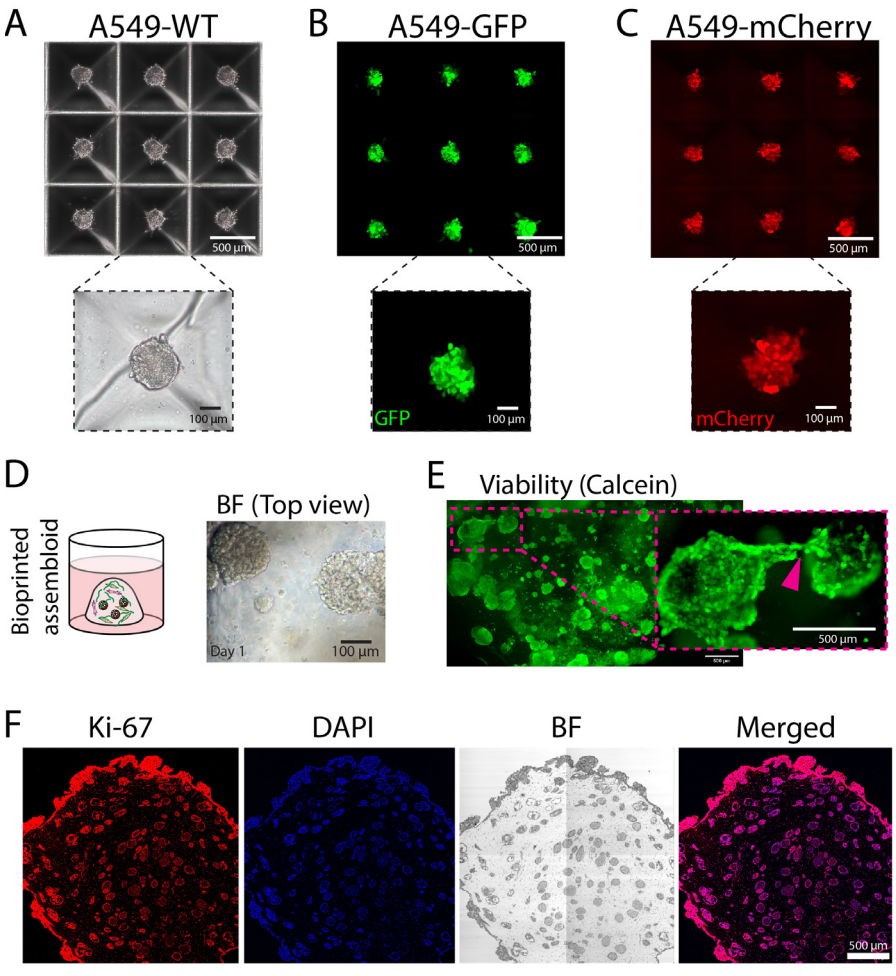

Figure 2. Viability and proliferation of lung cancer assembloids.
A-C) *Wild type and fluorescent (GFP- and mCherry-expressing) A549 cells were cultured in Sphericalplate 5D plates to grow hundreds of uniform cancer spheroids.*
D) *Cancer spheroids, HUVECs and CAFs were mixed with a custom bioink and bioprinted using the BIO X. Bright-field microscopy was used to observe structural integrity of the spheroids following the extrusion-based bioprinting.*
E) *Cellular viability was determined by staining with calcein. A day 7 image showed connecting spheroids (pink arrowhead).*
F) *Cellular proliferation was determined by immunostaining for Ki-67 of paraffin-embedded fixed assembloids on day 21. Scale bars are as indicated on individual images.*

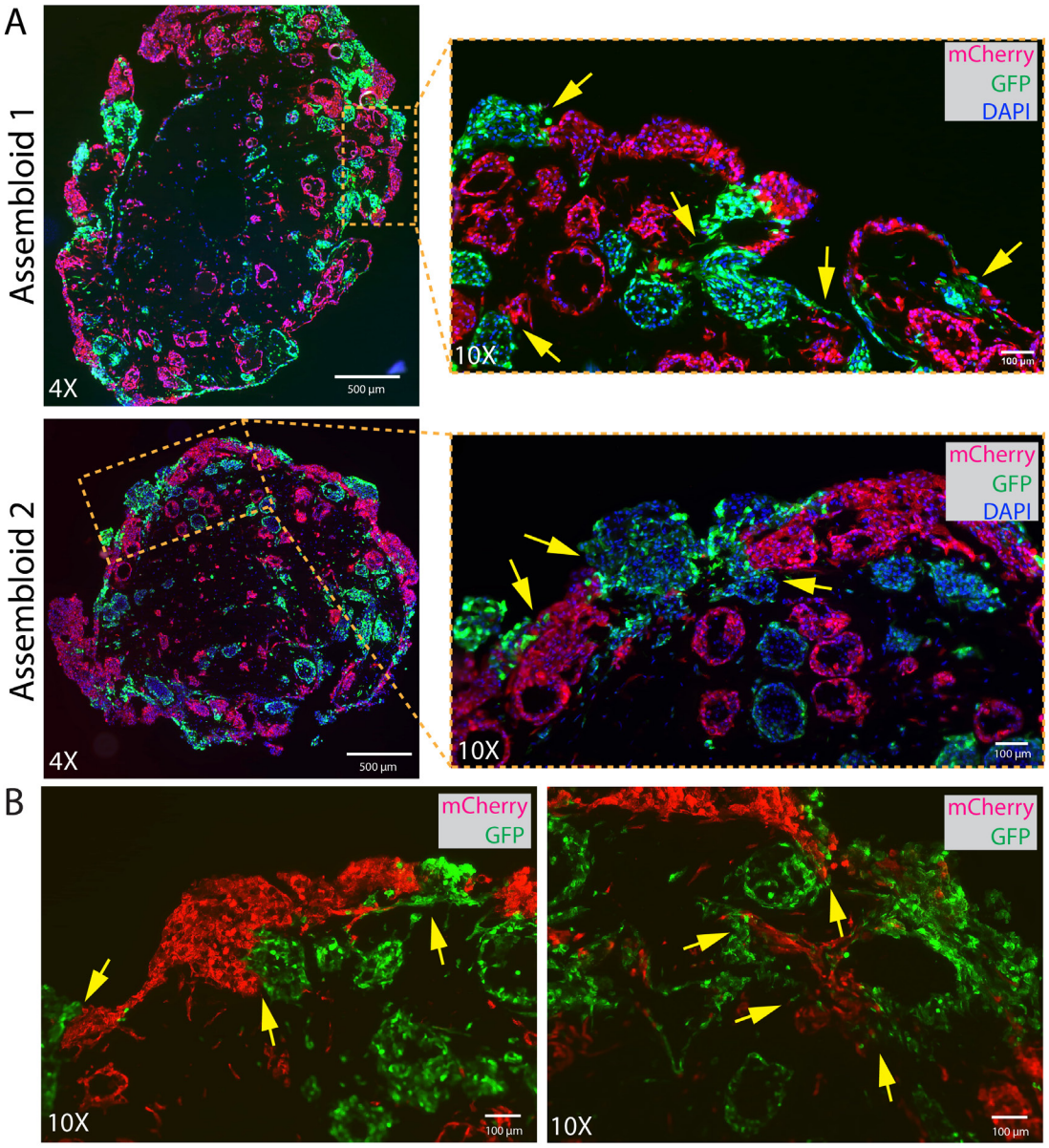

Figure 3. Migration of cells and fusion of spheroids. **A)** *Two replicates of fixed lung cancer assembloids containing GFP and mCherry-expressing A549 spheroids are shown. Fixed tissue slices were mounted with DAPI following deparaffinization.* **B)** *Magnified images of lung cancer assembloids with fluorescent A549 cells are shown without DAPI staining. Yellow arrows indicate cellular migration and fusion of spheroids. Scale bars are as indicated on individual images.*

Histology

To further confirm the fusion of spheroids and cellular migration, H&E staining was performed with the PFA-fixed paraffin-embedded assembloid tissues. **Figure 4** shows three lung cancer assembloid replicates that clearly depict merging spheroids (black arrowheads) within the assembloid structure. Interestingly, the micrographs also identify hollow alveolar lumen-like structures (green arrowheads) formed by A549 cells in the matrix. A similar observation was reported by another group (Abdul, 2020). Furthermore, a metastatic phenotype of A549 cells was observed where the cells were no longer confined within a spheroid. Rather, they seemed to leak out and propagate through the matrix (yellow circle and arrows).

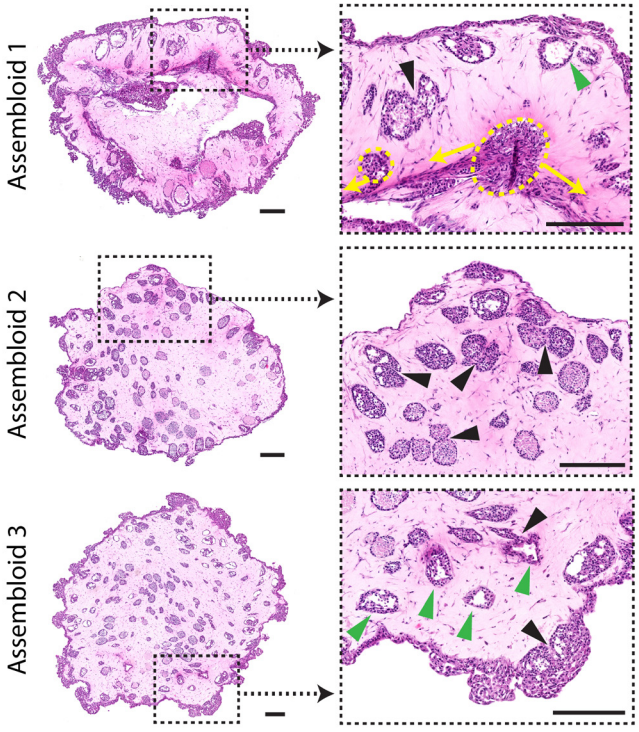

Figure 4. Histology of lung cancer assembloids. *H&E staining of three lung cancer assembloid replicates are shown. Green arrowheads indicate hollow alveolar lumen-like structures. Black arrowheads indicate fusion of spheroids. Yellow arrows indicate migration of cells from original spheroids (yellow circle) through the matrix. Scale bar = 250 µm.*

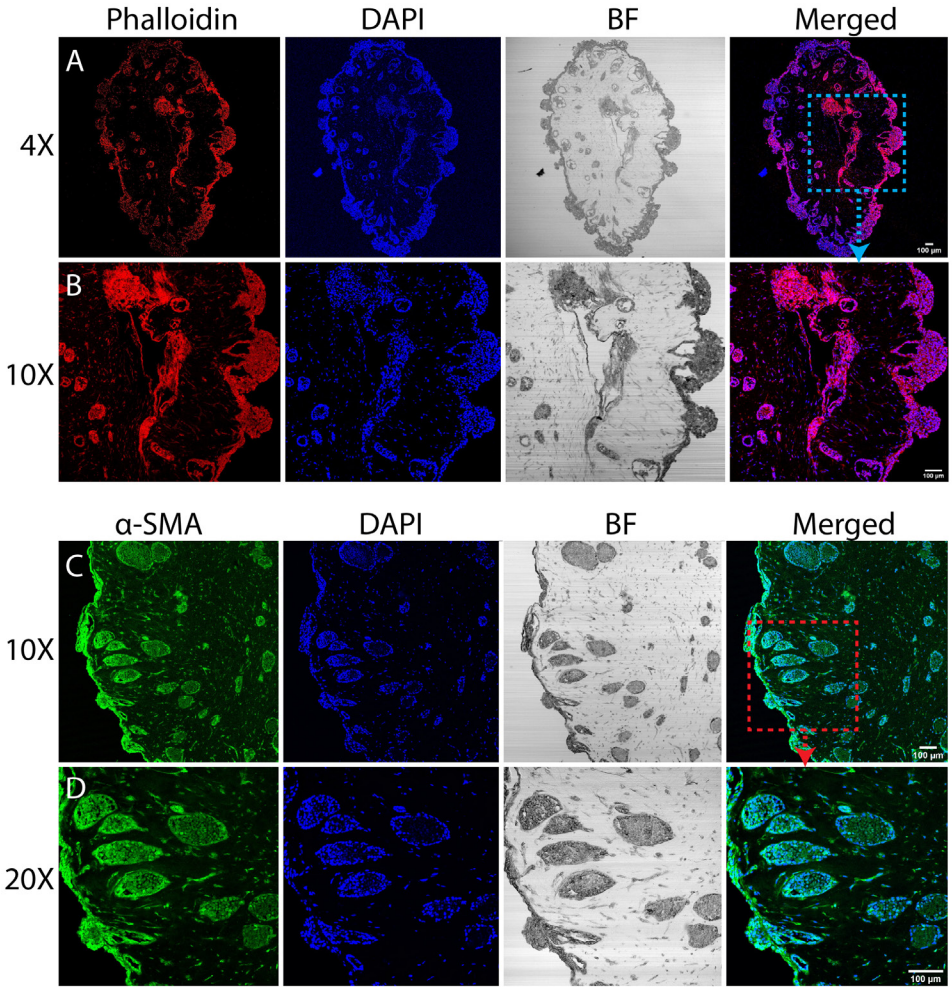

Figure 5. Expression of cytoskeletal markers.
A-B) *PFA-fixed, paraffin-embedded assembloids with wild type A549 cells were stained with Alexa647-conjugated phalloidin to visualize F-actin at different magnifications.*
C-D) *PFA-fixed, paraffin-embedded assembloids with wild type A549 cells were immunostained for α-SMA and counterstained with DAPI mounting agent. Corresponding bright-field images and merged images with DAPI are shown in the right two columns, respectively. Scale bars = 100 µm.*

Expression of cytoskeletal and adhesion marker

To examine the expression of cytoskeletal proteins by encapsulated cells, PFA-fixed and paraffin-embedded assembloids were stained for F-actin and α-SMA. **Figure 5** shows that the assembloid tissue expressed significant amounts of both F-actin and α-SMA. Similarly, **Figure 6** confirms the expression of several adhesion and cellular markers, such as vimentin, E-cadherin and CD93.

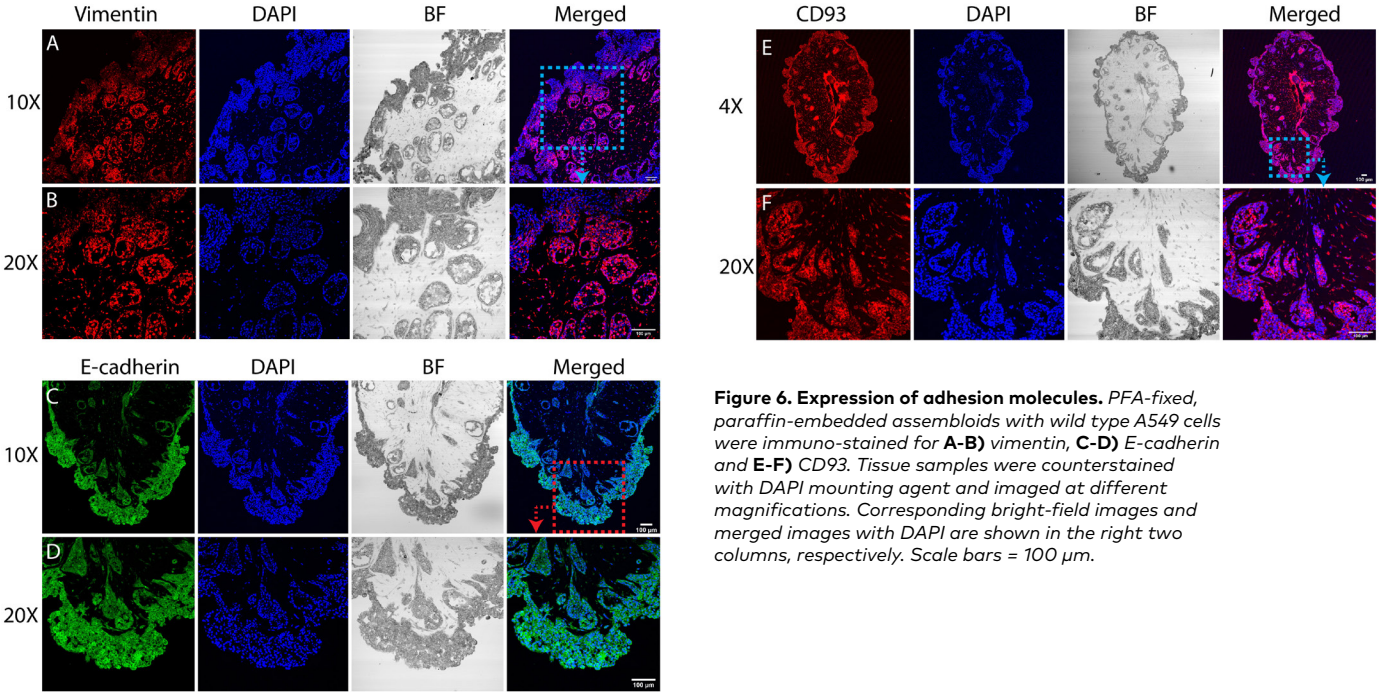

Figure 6. Expression of adhesion molecules. *PFA-fixed, paraffin-embedded assembloids with wild type A549 cells were immuno-stained for* **A-B)** *vimentin,* **C-D)** *E-cadherin and* **E-F)** *CD93. Tissue samples were counterstained with DAPI mounting agent and imaged at different magnifications. Corresponding bright-field images and merged images with DAPI are shown in the right two columns, respectively. Scale bars = 100 µm.*

Expression of immune checkpoint marker

Lung cancer cells are known to express high levels of immune checkpoint markers, such as PD-L1, which resulted in the clinical approval of anti-PD-L1 antibody as a first line immunotherapy treatment for lung cancer. To examine whether the lung cancer assembloids also expressed PD-L1, PFA-fixed assembloid tissue sections were immunostained with APC-conjugated anti-PD-L1 antibody and counterstained with DAPI mounting agent. Confocal imaging of the tissue showed high expression of PD-L1 on certain spheroids (**Figure 7**).

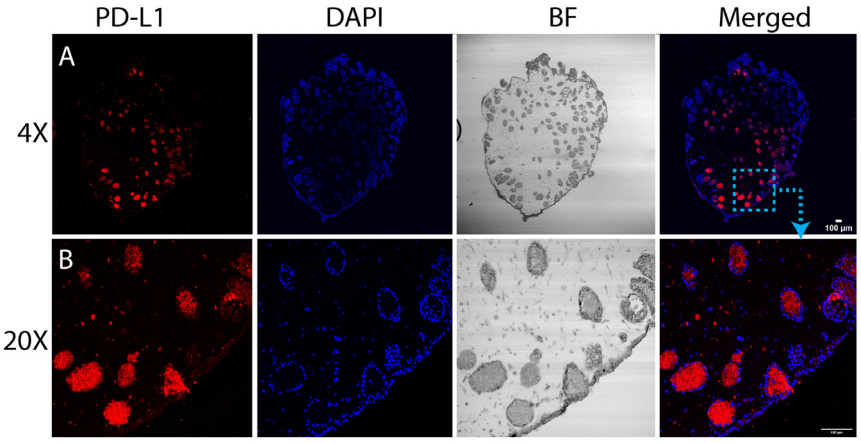

Figure 7. Expression of immune checkpoint marker. *PFA-fixed, paraffin-embedded assembloids with wild type A549 cells were immunostained for PD-L1. Tissue samples were counterstained with DAPI mounting agent and imaged at different magnifications. Corresponding bright-field images and merged images with DAPI are shown in the right two columns, respectively. Scale bars = 100 µm.*

Conclusions and future directions

In the present study, 3D bioprinted lung cancer assembloids were successfully developed by incorporating lung cancer cells, lung adenocarcinoma-associated fibroblasts and endothelial cells in a laminin-collagen-rich stromal environment. The following conclusions can be drawn from the study:

- The lung cancer assembloids exhibit characteristic spatial distribution of cytoskeletal proteins (F-actin and α-SMA) and adhesion molecules (E-cadherin, vimentin and CD93) that are found in real tumors.
- Histological analysis indicated multiregional architecture, spheroid fusion and formation of alveolar-like hollow lumen structures.
- The use of genetically encoded fluorescent cancer cells is a useful tool to visualize cellular migration and spheroid fusion.
- The embedded cancer cells also expressed PD-L1, implying the possible application of the assembloid model in *ex vivo* immunotherapy studies.

In this proof-of-concept study, a simple lung cancer assembloid model was developed and characterized. However, an in-depth study is warranted to investigate the roles of individual cell types and ECM components in drug-response studies. The model and analysis protocols described here can easily be adapted for other cancer and healthy tissue models to study oncology, developmental biology, drug development, regenerative medicine and toxicology, to name a few applications (**Figure 8**). Future directions include incorporating other stromal components, such as immune cells and functional microvasculature, into the assembloid structure and performing anti-cancer drug efficacy studies.

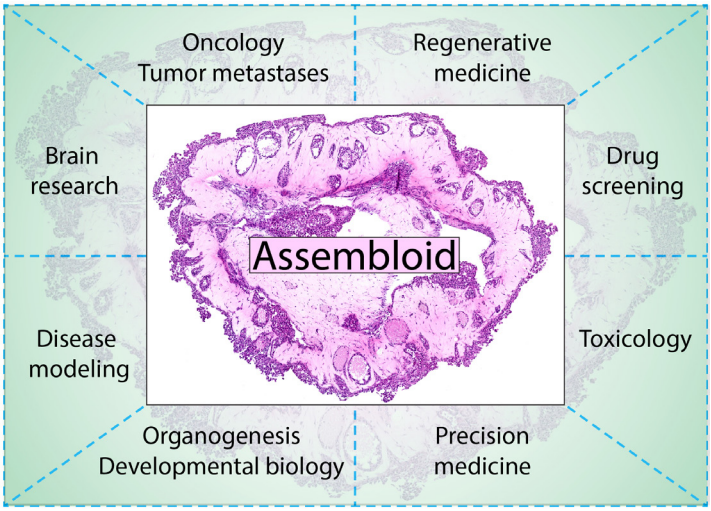

Figure 8. Application areas of assembloid model. *Assembloid models can easily be adapted for other cancer indications and healthy tissue types to study disease pathology, developmental biology, drug screening, regenerative medicine and toxicology, among others.*

References

1. Abdul L, Rajasekar S, Lin DSY, et al. Deep-LUMEN assay: Human lung epithelial spheroid classification from brightfield images using deep learning. *Lab on a Chip*. 2020; 20(24): 4623–4631. DOI:10.1039/D0LC01010C.

2. Andersen J, Revah O, Miura Y, et al. Generation of functional human 3D cortico-motor assembloids. *Cell*. 2020; 183(7): 1913–1929. DOI:10.1016/j.cell.2020.11.017.

3. Bissell MJ. Radisky D. Putting tumours in context. *Nature Reviews*. Cancer. 2001; 1(1): 46–54. DOI:10.1038/35094059.

4. Kercher EM, Nath S, Rizvi I, Spring BQ. Cancer cell-targeted and activatable photoimmunotherapy spares T cells in a 3D coculture model. *Photochemistry and Photobiology*. 2020; 96(2): 295–300. DOI:10.1111/php.13153.

5. Kim E, Choi S, Kang B. et al. Creation of bladder assembloids mimicking tissue regeneration and cancer. *Nature*. 2020; 588(7839): 664–669. DOI:10.1038/s41586-020-3034-x.

6. Marton RM, Pașca SP. Organoid and assembloid technologies for investigating cellular crosstalk in human brain development and disease. *Trends in Cell Biology*. 2020; 30(2): 133–143. DOI:10.1016/j.tcb.2019.11.004.

7. Miura Y, Li MY, Birey F. Generation of human striatal organoids and cortico-striatal assembloids from human pluripotent stem cells. *Nature Biotechnology*. 2020; 38(12): 1421–1430. DOI:10.1038/s41587-020-00763-w.

8. Sahai E, Astsaturov I, Cukierman E, et al. A framework for advancing our understanding of cancer-associated fibroblasts. *Nature Reviews Cancer*. 2020; 20(3): 174–186. DOI:10.1038/s41568-019-0238-1.

CONTACT US

Arvid Wallgrens Backe 20,
413 46 Gothenburg, Sweden

EU: +46 31-12 87 00
sales@cellink.com
www.cellink.com

155 Seaport Blvd, Unit 2B
Boston, MA 02210

US: +1 (833) 235-5465
sales@cellink.com
www.cellink.com

CELLINK
A BICO COMPANY